Makara J. Technol. 20/1 (2016), 19-23
doi: 10.7454/mst.v20i1.3051

Texture Analysis using The Neutron Diffraction Method on The Non Standardized Austenitic Steel Process by Machining, Annealing, and Rolling

Tri Hardi Priyanto[1*], Parikin[1], and Meijuan Li[2]

1. Center of Science and Technology for Advanced Materials, National Atomic Energy Agency/BATAN, Puspiptek Serpong, Banten 15314, Indonesia
2. Neutron Scattering Laboratory, China Institute of Atomic Energy, Beijing 10243, China

e-mail: thardi@batan.go.id

Abstract

Austenitic steel is one type of stainless steel which is widely used in the industry. Many studies on austenitic stainless steel have been performed to determine the physical properties using various types of equipment and methods. In this study, the neutron diffraction method is used to characterize the materials which have been made from minerals extracted from the mines in Indonesia. The materials consist of a granular ferro-scrap, nickel, ferro-chrome, ferro-manganese, and ferro-silicon added with a little titanium. Characterization of the materials was carried out in three processes, namely: machining, annealing, and rolling. Experimental results obtained from the machining process generally produces a texture in the ⟨100⟩ direction. From the machining to annealing process, the texture index decreases from 3.0164 to 2.434. Texture strength in the machining process (BA2N sample) is 8.13 mrd and it then decreases to 6.99 in the annealing process (A2DO sample). In the annealing process the three-component texture appears, cube-on-edge type texture {110}⟨001⟩, cube-type texture {001}⟨100⟩, and brass-type {110}⟨112⟩. The texture is very strong leading to the direction of orientation {100}⟨001⟩, while the {011}⟨100⟩ is weaker than that of the {001}, and texture with orientation {110}⟨112⟩ is weak. In the annealing process stress release occurred, and this was shown by more randomly pole compared to stress release by the machining process. In the rolling process a brass-type texture{110}⟨112⟩ with a spread towards the goss-type texture {110}⟨001⟩ appeared, and the brass component is markedly reinforced compared to the undeformed state (before rolling). Moreover, the presence of an additional {110} component was observed at the center of the (110) pole figure. The pole density of three components increases with the increasing degree of thickness reduction. By increasing degrees of rolling from 81% to 87%, the value of orientation distribution function increases by a factor about three times.

Abstrak

Analisis Tekstur Menggunakan Metode Difraksi Neutron pada Baja Austenite Non Standar yang Diproses dengan Permesinan, Penganilan, dan Pengerolan. Baja austenitik merupakan salah satu jenis baja tahan karat yang banyak digunakan dalam industri. Banyak studi telah dilakukan pada baja tahan karat austenitik dengan menggunakan berbagai jenis peralatan dan metode untuk menentukan sifat fisika. Dalam penelitian ini telah dibuat dari mineral yang diekstraksi dari tambang di Indonesia dan dikarakterisasi dengan metode difraksi neutron. Bahan terdiri dari butiran ferro-scrap, nikel, ferro-krom, ferro-mangan, dan ferro-silikon dan ditambahkan sedikit titanium. Karakterisasi bahan dilakukan dalam tiga proses, yaitu: proses permesinan, proses anil, dan proses pengerolan. Hasil eksperimen yang diperoleh dari proses pemesinan secara umum menghasilkan tekstur dalam arah ⟨100⟩. Dari proses permesinan ke proses anil indeks tekstur turun dari 3,0164 ke 2,434. Kekuatan tekstur dalam proses pemesinan (sampel BA2N) adalah 8,13 mrd kemudian turun menjadi 6,99 dalam proses anil (A2DO sampel). Dalam proses anil terlihat tiga komponen tekstur yaitu, tekstur jenis kubus-pada-tepi {110}⟨001⟩, tekstur jenis-kubus {001}⟨100⟩, dan tekstur jenis-kuningan {110}⟨112⟩. Tekstur yang sangat kuat terutama mempunyai arah orientasi {100}⟨001⟩, sedangkan orientasi {011}⟨100⟩, lebih lemah dibandingkan dengan {100}⟨001⟩, dan tekstur dengan orientasi {110}⟨112⟩ merupakan orientasi yang lemah. Dalam proses anil terjadi pelepasan tegangan yang ditunjukkan oleh pole yang lebih acak dibandingkan dengan pelepasan tegangan pada proses pemesinan. Dalam proses pengerolan tampak tekstur jenis kuningan {110}⟨112⟩ menyebar dengan mengarah pada tekstur jenis goss {110}⟨001⟩, dan komponen tekstur jenis kuningan nyata diperkuat dibandingkan dengan keadaan tak terdeformasi (sebelum pengerolan). Selain itu, adanya komponen tambahan {110} diamati di pusat pole figure (110). Kerapatan pole dari tiga komponen meningkat dengan meningkatnya tingkat pengurangan ketebalan. Dengan meningkatkan derajat pengerolan sebesar 81-87%, nilai fungsi distribusi orientasi meningkat dengan faktor sekitar tiga kali.

Keywords: austenitic stainless steel, neutron diffraction, texture

1. Introduction

Austenitic stainless steel types are the most widely used stainless steels which contain nominally 18% chromium and 8% nickel. These materials exhibits an attractive combination of good strength, ductility, toughness, excellent corrosion resistance, and good weldability. Due to these attributes, austenitic stainless steels are used in a range of industries, such as thermal power generation, biomedical and petrochemical, automotive, and chemical engineering [1]. Some shapes of stainless steel have been fabricated. Plat shapes of austenictic steels are conventionally manufactured by continuous casting, hot-rolling, subsequent cold-rolling, and final recrystallization [2]. The texture and microstructure of cold rolled and recrystallized austenitic stainless steels have already been subject to detailed investigations in the past. However, some subjects are still interesting to be investigated. Considering the deformation textures formed by cold-rolling, it is well known that a high Stacking Fault Energy (SFE) leads to a copper (or pure metal) type texture, whereas a lower SFE induces a brass (or silver, or alloy) type texture. The texture transition from the copper-type to the brass-type with decreasing SFE has been a highly controversial subject. Different microscopic mechanisms have been put forward to account for the copper-type texture (normal slip, cross slip, non-octaheral slip) and for the brass-type texture (normal slip, slip of partial dislocations, mechanical twinning [3]). Nevertheless, the problem remains still not well explained [4].

Some characterizations of stainless steel have also been performed using the neutron diffraction technique [5-6] and the quantitative texture analysis was carried out. The neutron diffraction technique is very useful because of the very small absorption of neutrons by metals, and this enables studying coarse-grained bulk samples. Using this technique absorption correction can be neglected and the possible variation of texture through the thickness of the sample can be integrated [4]. The comparison between the neutron diffraction measurements and the model predictions suggests that in most cases the finite model can predict the lattice strain evolution at the microscale and capture the general trends observed in the experiments [7]. The results associated with latent hardening effects at the microscale also indicate that in situ neutron diffraction measurements in conjunction with macroscopic uniaxial tensile data may be used to calibrate crystal plasticity models for the prediction of the inelastic material deformation response [8], for determining the retained austenite content of transformation induced plasticity (TRIP). With the complete orientation averaging the texture effect and with it the standard deviation of the austenite, mass fraction can be substantially reduced, regardless of the type or severity of the texture [6]. Residual strain measurements using neutron diffraction is also now a well-established method and its closely related to crystallite orientation (texture) measurement. The analysis of the uncertainty of the resultant strain and stress in residual stress measurement frequently brought into discussion is the accuracy of the final uncertainty of the measurement that is revisited and reassessed [9].

The purpose of this study is to characterize a non-standard austenitic stainless steel, which is made from extracts minerals in Indonesia [10], although the texture study of stainless steel has been performed with many instruments and methods, the characterization of non-standard austenitic steel using neutron diffraction is interesting to be performed under the influence of the mechanical processes, such as the machining, annealing, and rolling process.

Texture measurement and calculation. The crystallographic textures were quantitatively examined by measuring three incomplete {111}, {200}, and {220} pole figures using the neutron diffraction method. From the pole figures as two-dimensional projections of the texture, the three-dimensional orientation distribution function (ODF) was calculated using the William Imhoff Mathies Vinel (WIMV) method. In the case of cubic crystal symmetry and orthorhombic sample symmetry, which is set up by the rolling direction (RD), normal direction (ND), and transverse direction (TD), an orientation is represented by the three Euler angles φ_1, ϕ, and φ_2 in the reduced Euler space. For better transparency, an orientation is often presented in terms of the Miller indices (hkl) <uvw>, where it (hkl) describes the crystallographic plane which is parallel to the sheet surface and (uvw) the crystal direction that is parallel to RD. Because austenitic steels tend to develop characteristic fiber textures during rolling, it is convenient to depict the ODFs as iso-intensity diagrams in φ_2-sections through Euler space. In Figure 1, the most relevant fibers and orientations are displayed schematically [2].

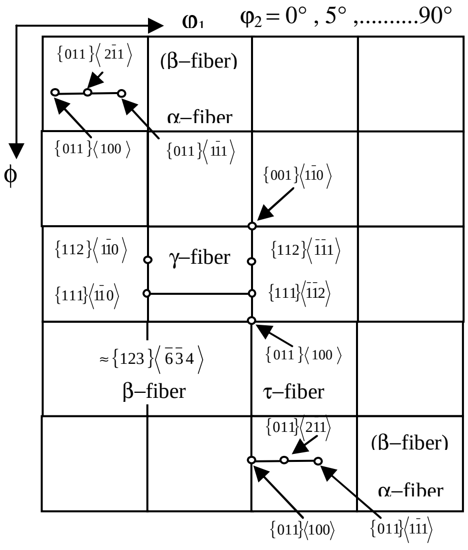

Figure 1. Some Relevant Orientation and Texture Fiber that Occur in Strip Cast & Hot-rolled Stainless Steels [2]

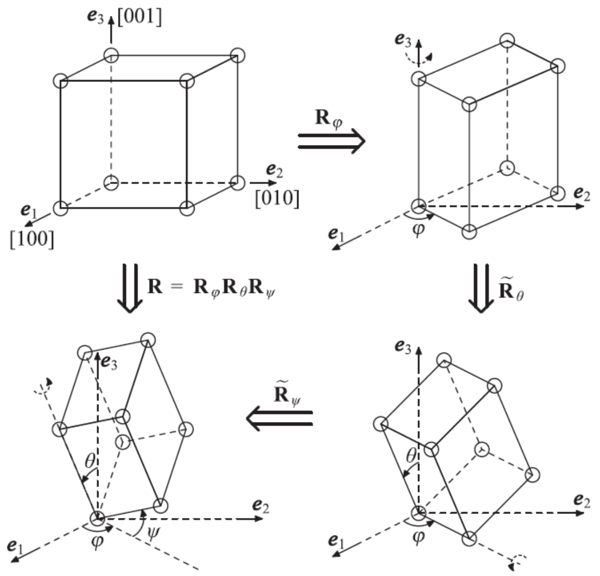

Figure 2. Schematic Ilustration of the Rigid Rotation Motion Operation in Euler Angles to Define the Crystallographic Orientation

α fiber: (110)｜｜ ND, main orientations:
$\{011\}\langle 100\rangle$, $\{011\}\langle 2\bar{1}1\rangle$, $\{011\}\langle 1\bar{1}1\rangle$, and $\{011\}\langle 0\bar{1}1\rangle$.
γ fiber: {111} ｜｜ ND, main orientations:
$\{111\}\langle 0\bar{1}1\rangle$ and $\{111\}\langle \bar{1}\bar{1}2\rangle$.
τ fiber:⟨110⟩｜｜ TD, main orientations:
$\{001\}\langle 0\bar{1}0\rangle$, $\{112\}\langle \bar{1}\bar{1}1\rangle$, $\{111\}\langle \bar{1}\bar{1}2\rangle$, and $\{011\}\langle 100\rangle$.
β fiber: less-symmetric-texture fiber containing the orientations: {11-2}⟨111⟩ (C), $\{123\}\langle \bar{6}\bar{3}4\rangle$(S), and $\{011\}\langle 2\bar{1}1\rangle$ (B).

2. Experiments

Synthesis of austenitic stainless steel with a material called A2 has been made in the Laboratory of Materials Synthesis PSTBM, BATAN Serpong. A2 raw material consists of a granular ferro-scrap, nickel, ferro-chrome, ferro-manganese, and ferro-silicon minerals extracted from the mines in Indonesia, and added with a little amount of titanium [10]. Low carbon content is maintained in the alloy ingot, and it is called the BA2N sample. Furthermore, three types of austenitic made from ingots BA2N, namely A2D0 prepared by the process of machining, and A2D3 and A2D4 samples that were made by the process of rolling with the different thickness reduction were prepared. The thickness reduction of A2D3 and A2D4 is about 81% and 87%, respectively. Furthermore, to restore the properties of materials as a result of rolling or to remove the texture properties, the material is air. Table 1 shows the specifications of the raw materials used to make steel nonstandard A2.

A three-dimensional analysis of texture was performed by computing the orientation distribution function (ODF), *F*(*g*), where *g*=[φ,Θ,Φ] represents the three Euler angles which a part of a given crystallite defined to the orientation with respect to the sample axes: normal direction ND, rolling direction RD, and transverse direction TD. The ODF was calculated using the William Imhoff Mathies Vinel (WIMV) method from three complete pole figures of {11l}, {200}, and {220}.

There are two samples, BA2N and A2D0 which have the same thickness of about 16 mm and after rolling A2D3 and A2D4 samples that have a thickness of about 6 mm. For the purposes of neutron diffraction experiments, two pieces of A2D3 sample were glued and sticked together in accordance with the rolling direction. This was done to obtain a thickness of about 12 mm, and the same use was applied to A2D4.

Pole figure measurements were taken for three Bragg peaks (111), (200), and (220). The sample was set with the normal direction (ND) parallel to the scattering vector at a position tilt angle = 90°, and the rolling direction (RD) in the vertical direction is perpendicular to the normal direction, while the transverse direction (TD) in the horizontal direction is perpendicular to the normal direction.

DN2 texture diffractometer was set at neutron wavelength λ=1.2799 Angstroms using a monochromator Si (311). The diffraction data were collected at an angle (ϕ,χ) in range from (0°,0°) to (360°,75°) using step scan (Δϕ,Δχ) = (5°,5°). Three pole figures of (111), (200), and (220) were obtained from the diffraction data for each sample.

3. Results and Discussion

Four types of samples, namely BA2N, A2D0, A2D3, and A2D4 with a different mechanical process, have been made and then characterized. The specification of raw materials is shown in Table 1.

Machining and annealing texture. The BA2N sample was produced from the machining process. It shows that because the machining process crystalites were oriented in ⟨100⟩ the direction with a texture index equal to 3.0164. Pole figures of the BA2N sample are shown in Figure 3. Three types of texture component can be interpreted as a cube-on edge type texture {110}⟨001⟩, cube type texture {001}⟨100⟩, and brass type {110}⟨112⟩. It is shown in Figure 3, that the texture is very strong leading with the direction of orientation {100}⟨100⟩,

Tabel 1. Specification of Raw Materials used for Non Standard Steel A2 [11]

Composition	Fe scrap (1)	FeCr (1)	FeMn (2)	FeSi (1)	Ni
Fe	99.17	28.49	23.04	24.71	-
Ni	-	-	-	-	99.99
Cr	-	70.46	-	-	-
Mn	0.49	-	75.00	-	-
Si	0.30	0.94	0.52	75.00	-
C	0.03	0.073	1.30	0.118	-
Al	-	-	-	0.14	-
S	-	0.01	0.006	0.023	-
P	-	0.03	0.13	0.005	-
Ti	0.001	0.004	-	0.015	-

(1) Low carbon (2) Middle carbon

while the {011}⟨100⟩ is weaker than that of the {100}⟨001⟩. Texture with orientation brass type {110}⟨112⟩ is weak.

In the annealed sample (A2D0), texture can be interpreted as a cube-on edge type texture {110}⟨001⟩ and cube type texture {001}⟨100⟩. It is almost similar with the machining process, however, texture strength decreases because stress release and brass type {110}⟨112⟩ disappear. Stress release occurs because of the annealing process. It would improve the softness, ductility, and toughness of the materials. The texture index decreases to 2.434. It is also shown that the maximum texture strength in the BA2N is 8.13 mrd, and then it decreases to 6.99 mrd in the A2DO sample. The existence of stress release on the A2DO sample is also indicated from the orientation distribution function (ODF) which dramatically decreases from 146.21 in the BA2N sample to 62.00 in the A2DO sample, and it has more random poles as shown in Figure 4.

Rolling texture. The rolling texture can be interpreted as being essentially a brass-type texture {110}⟨112⟩ as a dominant texture [12], and being more spread towards the Goss-type texture {110}⟨001⟩ by increasing the rolling process. The brass type component is markedly reinforced as compared to the undeformed state (before the rolling process). Moreover, the presence of the additional {110} component is observed at the centre of the {110) pole figure. The pole density of these three components increases with the increasing degree of thickness reduction. The texture index increases from 1.0375 to 1.1236 with the inreasing degree of the rolling process from 81% to 87%, respectively. From the calculation, for the samples A2D3 and A2D4, the ratio orientation distribution function of the maximum value of the minimum orientation distribution function is 3.795 and 10.538, respectively. From this it seems that

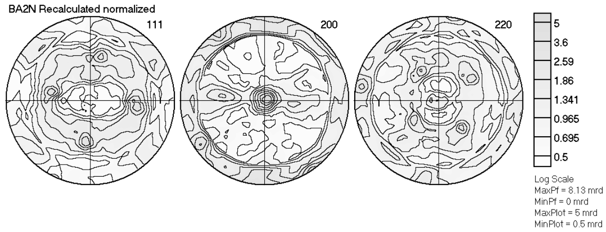

Figure 3. Normalized Pole Figures of (111), (200), and (220) for the BA2N Sample

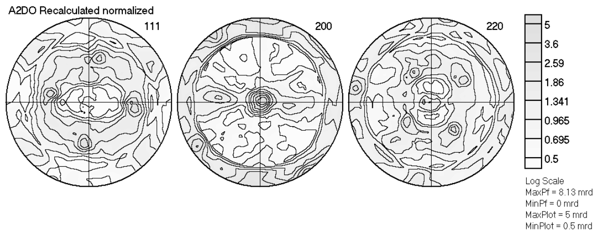

Figure 4. Normalized Pole Figures (111), (200), and (220) for the A2DO Sample

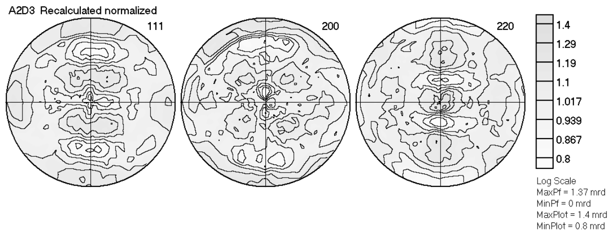

Figure 5. Normalized Pole Figures (111), (200), and (220) for the A2D3 Sample

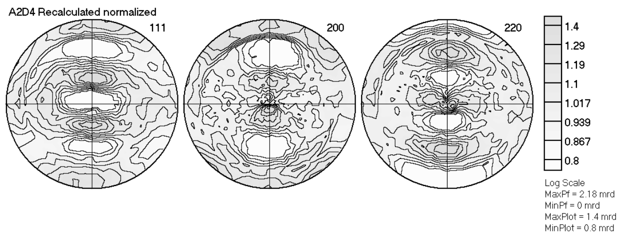

Figure 5. Normalized Pole Figures (111), (200), and (220) for the A2D4 Sample

the rolling effect is very influential in the orientation distribution function. By increasing the degree of rolling from 81% to 87%, the orientation distribution function increases about three times

Conclusion

From the results of a study on the steel material made from scrap materials, texture produced by the mechanical processes, such as machining, annealing, and rolling, can be summaried as follow.

Texture generated by the machining process produces three types of textures. They are cube-on-edge texture {110}⟨001⟩, cube-type {001}⟨100⟩, and brass-type {110}⟨112⟩, and the brass type has the weakest texture, while the cube-on-edge type is the strongest. In the annealing process stress release has occurred and resulted in the changes of crystal orientation, while brass type textures disappear. Compared to the machining process, texture index decreases from 8.13 to 6.99 mrd. Because of the rolling process, crystallite orientation leads into a brass-type {110}⟨112⟩ and becomes stronger with the increasing degree of rolling, and the increasing degree of rolling, the brass type texture {110}⟨112⟩ is dominant with spread towards to the Goss type orientation {110}⟨001⟩. By the increasing degrees of rolling, the value of orientation distribution function increases about three times.

Acknowledgements

The authors (THP) would like to thank to Bharoto M.Eng in the discussion and development of data acquisition programs for the texture analysis using DN2 texture diffractometer. The authors also would like to thank to Drs Nurdin Efendi, MSi who has made stainless steel materials from mineral material.

References

[1]. J. Sule, S. Ganguly, H. Coules, and T. Pirling, J. Manuf. Process. 18 (2015) 141.
[2]. D. Raabe, Metall. Mater. Trans. 26A (1995) 991.
[3]. M.N. Gussev, K.G. Field, J.T. Busby, J. Nucl. Mater. 460 (2015) 139.
[4]. C. Donadille, R. Valle, P. Dervin, R. Penelle, Acta Metall. 37/6 (1989) 1547.
[5]. V.I. Voronin, E.Z. Valiev, I.F. Berger, B.N. Goschitskii, N.V. Proskurnina, V.V. Sagaradze, N.F. Kataeva. J. Nucl. Mater. 459 (2015) 97.
[6]. T. Gnäupel-Herold, A. Creuziger, Mater. Sci. Eng. A, 528/10-11 (2011) 3594.
[7]. D.F. Li, N.P. O’Dowd, C.M. Davies, S.Y. Zhang, Eur. J. Mech. A/Solids. 30/5 (2011) 748.
[8]. D.F. Li, N.P. Odowd. J. Mech. Phys. Solids. 59/12, (2011) 2421.
[9]. R.C. Wimpory, M. Boin. Procedia Eng. 10 (2011) 1639.
[10]. T.H. Priyanto, Parikin, N. Efendi. Adv. Mater. Res. 1123 (2015) 1104.
[11]. Parikin, T.H. Priyanto, A.H. Ismoyo, N. Effendi, I. Wahyono. Urania. 20/2 (2014) 67.
[12]. T. Morikawa, K. Higashida. Mater. Trans. 51/4 (2010) 620.